Molecular Crystals and Liquid Crystals
Publication details, including instructions for authors and subscription information:
http://www.tandfonline.com/loi/gmcl16

Spin Susceptibilities and Phase Transitions in Some Simple Alkali-TCNQ Salts

Johan G. Vegter [a] & Jan Kommandeur [a]
[a] Laboratory for Physical Chemistry, The University, Groningen, The Netherlands
Version of record first published: 21 Mar 2007.

To cite this article: Johan G. Vegter & Jan Kommandeur (1975): Spin Susceptibilities and Phase Transitions in Some Simple Alkali-TCNQ Salts, Molecular Crystals and Liquid Crystals, 30:1-2, 11-49

To link to this article: http://dx.doi.org/10.1080/15421407508082839

Mol. Cryst. Liq. Cryst., 1975, Vol. 30, pp. 11–49

Printed in Holland

Spin Susceptibilities and Phase Transitions in Some Simple Alkali-TCNQ Salts

JOHAN G. VEGTER and JAN KOMMANDEUR

Laboratory for Physical Chemistry, The University, Groningen, The Netherlands

(*Received March 11, 1974*)

Spin susceptibility measurements in crystalline alkali$^+$TCNQ$^-$ salts reveal the occurrence of continuous changes and first-order phase transitions in these salts, except Li$^+$TCNQ$^-$. A consideration of the total free energy of these distorted linear systems, in which the electronic energy results from an elementary one-dimensional split band model, leads to a temperature dependent band gap and band width and readily predicts these structural changes, induced by the electronic system. The outlines of the theory are given first on a more symmetrical model, which leads to first- and second-order semiconductor-to-metal transitions. Calculations were performed in detail on the basis of the accurately known crystal structure of Rb$^+$TCNQ$^-$, which lead to first-order semiconductor-to-semiconductor transitions, as observed. The experimental absolute susceptibility data, arising from the low temperature as well as from the high temperature phase, are compared successfully with predictions from the theoretical model.

I. INTRODUCTION

In a recent paper Vegter, Fedders and Kommandeur[1] described the susceptibility behavior of crystalline LiTCNQ in terms of a simple one-dimensional split band theory, using the tight-binding approximation for the extra electron on each TCNQ$^-$ ion. In a stoichiometric crystal all electrons can be accommodated in the lower band at 0°K. In reference 1, hereafter I, the applicability of band theory is discussed and the theory is worked out in detail. The temperature variation of the Fermi energy and spin susceptibility is calculated and compared successfully with the experimental susceptibility data of some LiTCNQ samples.

The application of this simple band theory to the other pseudo-one-dimensional (1:1) alkali TCNQ-ides M$^+$TCNQ$^-$ (M $\neq$ Li) was hampered by the occurrence of phase transitions. These transitions, experimentally

observed by measuring the temperature dependence of spin susceptibility, d.c.-conductivity and X-ray diffraction and confirmed by the heats of transition involved, were reported by Vegter, Hibma and Kommandeur.[2]

Because the energy gap in the symmetry-split band system is strongly dependent on the amount of distortion ("dimerization") of a $TCNQ^-$ chain and because of the narrowness of the electronic energy bands in these solids (see I), small structural changes may lead to drastic changes in the electronic spin- and partition-entropy and consequently in the electronic free energy of the crystal. As will be shown in section IV, a detailed consideration of the total free energy of an M^+TCNQ^- crystal, based on the known crystal structure of RbTCNQ,[3] as a function of volume, temperature and degree of distortion of a $TCNQ^-$ chain, results in a temperature dependent energy gap between the bands. In warming up the crystal a continuous structural change occurs, possibly followed by a first-order phase transition, leading to an almost constant gap at higher temperatures. Therefore the unperturbed band theory, i.e. with constant band parameters, as applied to LiTCNQ in I, also holds for the high temperature phase in most other M^+TCNQ^- salts. On the other hand, in the low temperature phase the dependence of energy gap on temperature strongly affects the behavior of the susceptibility as a function of temperature for instance. Spin susceptibilities, calculated on this basis, will be compared with experimental data in section V.

Due to the asymmetrical, but electrostatically very stable, geometry within each chain in the RbTCNQ crystal (see figures 5 and 6 in ref. 3), the above mentioned transitions are first-order semiconductor-to-semiconductor transitions. However, first of all, the outlines of the theory will be given in an approximate treatment on a more symmetrical model (section II). At low temperatures the "dimerization" of $TCNQ^-$ ions along a chain will be discussed, together with its instability at higher temperatures, leading to a transition from a split band to a single band situation. In this simplified model, we are concerned with first- or second-order semiconductor-to-metal transitions, depending on the ratio between the electronic binding energy and the deformation energy of the rigid lattice. This electronically induced crystallographic nonmetal-metal transition was discussed earlier by Adler and Brooks[4] and Hallers and Vertogen.[5] They considered a linear chain of delta-function potentials and neglecting overlap, arrived at second-order phase transitions only, in contrast to the present treatment, which leads to first-order or second-order phase changes.

A detailed discussion of the order of the semiconductor-to-metal and semiconductor-to-semiconductor phase changes, with reference to Landau's theory for second-order transitions,[6] will be given elsewhere,[7] but some remarks to this point are given in section III.

II. APPROXIMATE TREATMENT

(a) The simplified model

The known crystal structure of RbTCNQ[3] as well as the preliminary structural data of KTCNQ[8] point to linear chains of $TCNQ^-$ ions, surrounded by positive ions, in the M^+TCNQ^- crystals. The electronic interaction between adjacent chains is supposed to be negligible in these salts. Therefore the electronic properties will again be described by a simple one-dimensional band theory, as presented by Fedders and Kommandeur[9] and worked out in I.

Let us consider two simplified representations of N $TCNQ^-$ ions within a linear row, as given in figure 1. The $TCNQ^-$ ion radicals, which are taken to be planar, are perpendicular to the plane of the paper. In figure 1A we have one ion per one-dimensional unit cell (length: $\frac{1}{2}a$), which leads to one half-filled metallic band at 0°K if Bloch theory is applied to the "valence orbital" (half-filled orbital) of the $TCNQ^-$ ion.

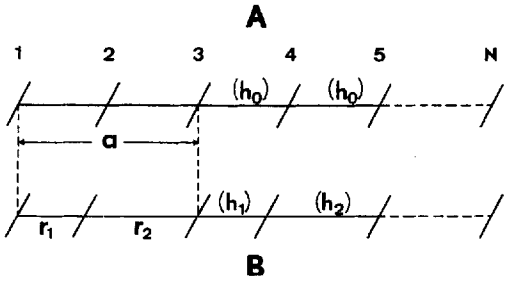

FIGURE 1 Simplified representation of N $TCNQ^-$ ions within a linear row;
A. Undistorted structure
B. Distorted structure.

The major interaction in this one electron theory is given by the transfer integral h between neighboring radicals

$$h_{1,2} = \int \varphi^*_{1,2} V' \varphi_0 \, d\tau \tag{2.1}$$

In this expression V' is the lattice potential deriving from all sites except the site labeled 0. The φ's are π-electron wavefunctions for the unpaired electrons in the $TCNQ^-$ ions. If we have one ion per unit cell ($h_1 = h_2 \equiv h_0$), the energy is given by

$$E^{\pm}(k) = \pm E_c |\cos(\tfrac{1}{2}ak)| \tag{2.2}$$

where $E_c = 2|h_0|$.

However, the low temperature structure of RbTCNQ (figure 5) exhibits a certain degree of structural distortion, which gives the appearance of dimers along a chain, as depicted in a simple manner in figure 1B. The distances between successive $TCNQ^-$ ions alternate between r_1 and r_2, so we have two ions per unit cell (length: a), and the band picture looks like figure 2, in which the bandgap $2E_g$ appears as a result of the decrease of symmetry. All electrons will be accommodated in the lower band at 0°K.

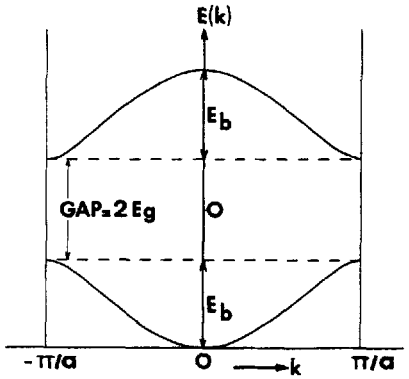

FIGURE 2 Split-band system in the reduced zone scheme for a one-dimensional distorted chain.

We define an alternation parameter ξ, which gives us the degree of distortion:

$$\xi \equiv \frac{r_2 - r_1}{r_2 + r_1} = \frac{r_2 - r_1}{a} \quad \text{or } r_{1,2} = \tfrac{1}{2}a(1 \mp \xi) \text{ with } 0 \leq |\xi| < 1 \tag{2.3}$$

In practice $|\xi| \ll 1$ ($\lesssim 0.1$).

The band energies were derived in I and are given by

$$E^{\pm}(k) = \pm E_c(g^2 + \cos^2(\tfrac{1}{2}ak))^{1/2} \tag{2.4}$$

in which

$$E_c = 2|h_1 h_2|^{1/2} \tag{2.5}$$

and

$$g = \frac{|h_1| - |h_2|}{2(h_2 h_2)^{1/2}} = \sinh\left(\tfrac{1}{2}\ln\left|\frac{h_1}{h_2}\right|\right) \tag{2.6}$$

Furthermore the width of each band is

$$E_b = 2|h_2|, \quad \text{with } |h_2| < |h_1| \tag{2.7}$$

In this dimerlike picture h_1 and h_2 are transfer integrals between a radical and its two inequivalent neighbors.

We now want to discuss the occurrence of a lattice distortion ($\xi \neq 0$) at low temperatures and its disappearance ($\xi = 0$) at higher temperatures.

(b) "Dimerization" at low temperatures

Starting from the highly symmetrical structure given in figure 1A, it may be quite imaginable that a certain degree of dimerization (figure 1B) will result in a gain of electronic energy, which exceeds the loss in elastic energy. At very low temperatures entropy contributions do not enter into the problem, so a gain in total energy will result in a spontaneous distortion.

We will calculate the electronic and elastic energy contributions at 0°K in a stoichiometric crystal. For this purpose we need an expression for the transfer integrals in terms of known quantities. Because neighboring radicals are well separated ($\frac{1}{2}a \approx 3.5$Å), this can be done by substituting a Coulombic interaction potential e^2/r for the potential energy operator in (2.1) and by writing the π-electron wavefunctions as atomic $2p\sigma$-functions with an effective nuclear charge $Z' = 3.4$ as used by Jonkman and Kommandeur in their SCMO-CI calculations on $TCNQ^0$, $TCNQ^-$ and $TCNQ^{=}$.[10] With these approximations we arrive at

$$h_{1,2} \approx \frac{Z'}{12}(cr_{1,2})^3 \exp(-cr_{1,2}) = \text{const.}\, r_{1,2}^3 \exp(-cr_{1,2}) \tag{2.8}$$

where $c = Z'/2a_0'$ and a_0' is the Bohr radius. We suppose that at least the dependence on distance is adequately given by (2.8); for the present we will not attach great value to the pre-exponential constant. Insertion of (2.3) into (2.8) gives

$$h_{1,2} = h_0(1 \mp \xi)^3 \exp(\pm \tfrac{1}{2}ac\xi) \tag{2.9}$$

Substitution of (2.9) into (2.5)

$$E_c = 2|h_0|(1 - \xi^2)^3 \approx 2|h_0| \tag{2.10}$$

almost independent of the amount of distortion.

Combining (2.6) and (2.9)

$$g \approx \sinh((\tfrac{1}{2}ac - 3)\xi) \approx (\tfrac{1}{2}ac - 3)\xi \tag{2.11}$$

which indicates that the energy gap $2E_g = 2E_c|g|$ is practically directly proportional to the degree of alternation ξ. With the aid of these formulas the difference in electronic energy between the structures A and B in figure 1 can be calculated. In a crystal (volume V) containing N radical ions the

energies in question are

$$E_{el}(A) = -E_c \sum_k |\cos(\tfrac{1}{2}ak)| = -\frac{NE_c}{\pi}\int_{-\pi/2}^{\pi/2} |\cos(\tfrac{1}{2}ak)|\, d(\tfrac{1}{2}ak) = -\frac{2}{\pi}NE_c$$

$$E_{el}(B) = -E_c \sum_k (g^2 + \cos^2(\tfrac{1}{2}ak))^{1/2} \tag{2.12}$$

$$= -N\frac{E_c}{\pi}\int_{-\pi/2}^{\pi/2} (g^2 + \cos^2(\tfrac{1}{2}ak))^{1/2}\, d(\tfrac{1}{2}ak) \approx -NE_c(g^2 + 4/\pi^2)^{1/2}$$

The summations are taken over all occupied states. The final expression for $E_{el}(B)$ was obtained via an appropriate approximation of a complete elliptic integral of the second kind in the limit of low $|g|$ values. The gain in electronic energy amounts to

$$\Delta E_{el}(\xi) = E_{el}(B) - E_{el}(A) = -\frac{2}{\pi}NE_c(\sqrt{1 + \tfrac{1}{4}\pi^2 g^2} - 1)$$
$$\approx -\tfrac{1}{4}\pi g^2 NE_c \equiv -\tfrac{1}{2}V\kappa_{el}^{-1}(0)\xi^2 \tag{2.13}$$

We have rewritten this expression as a parabolic compressibility term, in which $\kappa_{el}^{-1}(0)$ may be regarded as the "compressibility of the valence electrons" at 0°K, which is negative owing to the attractive nature of this electronic energy.

It is worthwhile for a moment to consider the behavior of the integral in (2.12) in the limit of $g = 0$. It can then be shown that this integral and therefore $\kappa_{el}^{-1}(0)$ goes to infinity and, in contrast with the result of Adler and Brooks,[4] an infinitesimally small distortion will always appear at 0°K, irrespective of the magnitude of the lattice compressibility. This singularity in κ_{el}^{-1} is related to the infinite density of states at the band edges, which is merely due to the one-dimensionality of the problem. The latter singularity is removed by taking into account the three-dimensionality of the crystal. The energy contours in **k**-space will no longer be perfect parallel planes perpendicular to the k_x-axis, as in the purely one-dimensional model. Due to the (very small) interchain interactions the constant energy surfaces will not be quite planar. Now, an infinitesimally small distortion at 0°K results in a gap, which does not open up along the whole Fermi energy surface at once, but we are left with two energy bands with small partial overlap. The crystal remains "metallic" and the above mentioned singularity in κ_{el}^{-1} disappears. The complete separation of both bands is attained at somewhat larger distortions. Expression (2.12) for the electronic energy can in this limit be retained by replacing the upper limit of the integration by $\pi/2 - \varepsilon$, where ε is a small number, which measures the ratio of the interchain interactions. This change of the limit of integration removes the necessity for

considering the integral in the limit of $g = 0$; it only has to be studied for small values of g. In this case, we can approximate the energy by (2.13). Using (2.13) and (2.11) we find

$$\kappa_{el}^{-1}(0) = \tfrac{1}{2}\pi(\tfrac{1}{2}ac - 3)^2 E_c N/V \tag{2.14}$$

$E_c/k \approx 1500°\text{K}$ appears to be a representative value in M^+TCNQ^- crystals (see section V). Together with $\frac{1}{2}ac \approx 11$ and $N/V \approx 3.5 \times 10^{21}\ \text{cm}^{-3}$ we calculate

$$\kappa_{el}(0) \approx 1.4 \times 10^{-11}\ \text{cm}^2/\text{dyne} \tag{2.15}$$

The loss in elastic energy of the rigid lattice may be written in an analogous way for small ξ:

$$\Delta E_l(\xi) = \tfrac{1}{2}V\kappa_\xi^{-1}\xi^2 \tag{2.16}$$

in which the "alternation compressibility" κ_ξ will not differ much from the linear compressibility κ_l of the rigid, ionic lattice, along the stacking axis of the crystal. This is confirmed by detailed calculations on the basis of the known RbTCNQ structure (section IV). It will be found there that

$$\kappa_\xi(\approx \kappa_l) \approx 2.4 \times 10^{-11}\ \text{cm}^2/\text{dyne} \tag{2.17}$$

The "dimerized" structure (B) will be in favor at 0°K if

$$\kappa_\xi^{-1} - \kappa_{el}(0) < 0, \quad \text{or} \quad \kappa_\xi > \kappa_{el}(0) \tag{2.18}$$

The dependence of energy on ξ is depicted in figure 3, in which both energy

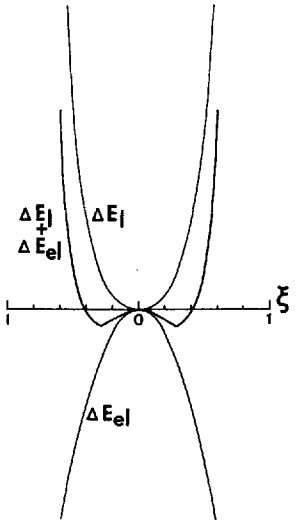

FIGURE 3 Dependence of the deformation energy ΔE_l, the electronic energy ΔE_{el} and the total energy $\Delta E_l + \Delta E_{el}$ on the distortion parameter ξ at 0°K, in the case $\kappa_\xi > \kappa_{el}(0)$.

contributions are plotted against ξ. The lattice energy expression (2.16) only holds in the limit of low alternation; at higher ξ-values the intrachain repulsive forces will cause a sharp rise in ΔE_1. Besides this, the gain in electronic energy at larger distortions is overestimated by the simple quadratic expression (2.13). The combination of these effects will cause an equilibrium distortion, which will be achieved at the minimum of total energy at 0°K.

Whether the above mentioned rearrangement of molecules occurs or not, completely depends upon *both* compressibilities. If we are dealing with a more rigid lattice (decreasing κ_ξ) or a smaller interaction of the valence electrons (decreasing E_c), the lattice energy will dominate the total energy and dimerization becomes impossible.

Finally, it should be noted that the feature of stabilizing a structural distortion is not merely a property of a band system as discussed above, but rather must be regarded as a band generalization of the Jahn–Teller effect.

(c) The semiconductor-to-metal transition

Starting from the partly dimerized structure B (figure 1) we will examine its temperature dependence from figure 2. At a temperature T electrons will be excited from the lower to the upper band and the excitation density will be roughly proportional to $\exp(-E_g/kT)$. Although each excitation means an energy loss, it is accompanied by an entropy gain, due to the partition of electron and hole over the various energy levels as well as the resulting spin entropy. This entropy term can be enhanced by reducing the gap between both bands in figure 2, resulting in an increase of the excitation density. However, in its turn, this is counteracted by the energy lift of the almost completely filled lower band. This competition between the entropy (S) and energy contributions, is of course described by the total free energy of the system $F = E - TS$, in which the lattice energy also plays a rôle. For the time being we neglect the free energy of the lattice vibrations, because the alternation parameter only enters it through the anharmonic terms. Furthermore we consider a constant external pressure and neglect any effect of crystal expansion.

At higher temperatures the entropy term in F becomes more and more important and a temperature dependent energy gap is not surprising. Finally the gap completely disappears and a transformation to structure A takes place (semiconductor-to-metal transition), which is first- or second-order in nature.

The disappearance of alternation, qualitatively argued above, will be treated in a quantitative manner below by considering the total free energy of the crystal as a function of alternation and temperature. The equilibrium

condition is

$$(\partial F(\xi, T)/\partial \xi)_T = 0 \tag{2.19}$$

The electronic free energy of the (stoichiometric) crystal can be derived from the partition function Z_{el} of the band system under consideration[11]

$$Z_{el} = \prod_k \{1 + \exp(-E^-(k)/kT)\}^2\{1 + \exp(-E^+(k)/kT)\}^2 \tag{2.20}$$

$E^{\pm}(k)$ are the single particle energies of the state k in the upper and lower band.

First of all we consider the simplified case of a split-band system, in which equal energies are given to all states belonging to the same band, while retaining the width of each band to some extent (cf. equation 2.12)

$$E^{\pm} = \pm E_c\left(g^2 + \frac{4}{\pi^2}\right)^{1/2} \tag{2.21}$$

Insertion of (2.21) into (2.20) gives

$$F_{el}^{(\xi, T)} = -kT \ln Z_{el} = -NE_c\left(g^2 + \frac{4}{\pi^2}\right)^{1/2} + \\ -2NkT \ln\left\{1 + \exp\left(-\frac{E_c}{kT}\left(g^2 + \frac{4}{\pi^2}\right)^{1/2}\right)\right\} \tag{2.22}$$

The first term clearly gives the electronic energy at 0°K, whereas the entropy contributions are contained in the temperature dependent term. The elastic (free) energy of the rigid lattice is again given by expression (2.16) and should be added.

Application of the equilibrium condition (2.19) gives as one solution the relationship between the amount of distortion and temperature

$$\left(1 + \exp\left\{\frac{E_c}{kT}\left(g^2 + \frac{4}{\pi^2}\right)^{1/2}\right\}\right)^{-1} = \frac{1}{2}\left\{1 - \left(1 + \frac{1}{4}\pi^2 g^2\right)^{1/2} \cdot \frac{\kappa_{el}(0)}{\kappa_\xi}\right\} \tag{2.23}$$

$\kappa_{el}(0)$ is defined earlier in (2.14).

The other solution of (2.19) is trivial

$$\xi = 0 \tag{2.24}$$

the undistorted lattice.

Solutions of (2.23) correspond with the "dimerized" phase and only exist if $\kappa_{el}(0) < \kappa_\xi$ (cf. equation 2.18).

At very low temperatures the system will take on a distortion $g(0) = \pm 2/\pi((\kappa_\xi/\kappa_{el})^2 - 1)^{1/2}$, which decreases at higher temperatures and vanishes

($g = 0$) at the transition temperature

$$T_t = \frac{2}{\pi}\left(\frac{E_c}{k}\right)\left[\ln\left(\frac{\kappa_\xi + \kappa_{el}(0)}{\kappa_\xi - \kappa_{el}(0)}\right)\right]^{-1}.$$

For $T > T_t$ only one solution remains, corresponding with $\xi = 0$, the metallic phase.

The above mentioned values of $\kappa_{el}^{(0)}$, κ_ξ and E_c were substituted in (2.23) and the resulting temperature dependence of the parameter $|g|$ is illustrated in figure 4. The lattice distortion is approximately directly proportional to g, as is the energy gap between both bands; therefore these quantities will show the same temperature behavior.

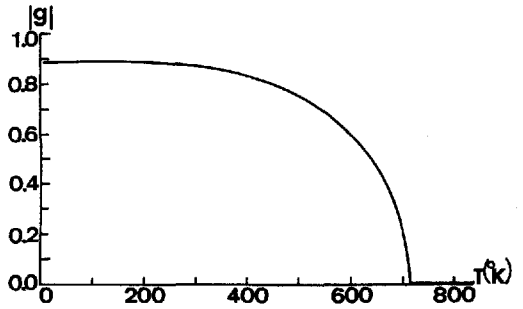

FIGURE 4 Behavior of g with temperature in the approximate treatment, leading to a second-order semiconductor-to-metal transition, calculated with $E_c/k = 1500°K$, $\kappa_{el}(0) = 1.4 \times 10^{-11}$ cm^2/dyne and $\kappa_\xi = 2.4 \times 10^{-11}$ cm^2/dyne. Energy band gap and lattice distortion are directly proportional to g in this treatment.

III. THE ORDER OF THE TRANSITION

Since there has been considerable discussion of the order of the semiconductor-to-metal transition[1,2,4,5] we will now devote a few remarks to that point. Moreover, the particular ordering of the TCNQ-chains precludes the introduction of an extra symmetry element. This, as we will show, transforms the second-order phase transitions into continuous changes within one phase.[6,13]

(a) The symmetrical case

In the approximate treatment given above, a symmetry element is added to the system, when it changes from semiconductor to metal. Therefore, it can always be stated, whether the material is in one phase or the other. There can then be first- or second-order phase changes. Let us consider

what orders of phase changes are predicted by the simplified model of section IIc.

Let us look at the curvature of the $F(\xi)$ curve in figure 3 near the transition point. It will be clear that a second-order transition from the semiconductive state (free energy minima at $\xi \neq 0$ and maximum at $\xi = 0$) to the metallic state. (minimum at $\xi = 0$) will require

$$(\partial^2 F(\xi, T)/\partial \xi^2)_{T=T_t} = 0 \tag{3.1}$$

The second derivative of the total free energy with respect to ξ reads

$$\left(\frac{\partial^2 F}{\partial \xi^2}\right)_T = V\kappa_\xi^{-1} - V\kappa_{el}^{-1}(0)(1 + \tfrac{1}{4}\pi^2 g^2)^{-3/2} \times \left\{1 + \frac{2e^{Q'}}{(1 + e^{Q'})^2}(\tfrac{1}{4}\pi^2 g^2 Q' - (1 + e^{-Q'}))\right\} \tag{3.2}$$

where

$$Q' \equiv \frac{E_c}{kT}\left(g^2 + \frac{4}{\pi^2}\right)^{1/2}.$$

At $\xi = 0$ this expression changes into:

$$\left(\left(\frac{\partial^2 F(\xi, T)}{\partial \xi^2}\right)_T\right)_{\xi=0} = V\kappa_\xi^{-1} - V\kappa_{el}^{-1}(0)\left\{1 - 2\left(1 + \exp\left(\frac{2E_c}{\pi kT}\right)\right)^{-1}\right\} \tag{3.3}$$

which indeed equals zero at

$$T = T_t = \frac{2}{\pi}\left(\frac{E_c}{k}\right)\ln^{-1}\left(\frac{\kappa_\xi + \kappa_{el}(0)}{\kappa_\xi - \kappa_{el}(0)}\right).$$

At $T < T_t$ $\xi = 0$ will be a maximum in $F(\xi)$ if $\kappa_\xi > \kappa_{el}(0)$ ("dimerization"), whereas at $T > T_t$ it is a minimum corresponding to the equilibrium position in the high temperature, metallic phase. Therefore, the simplified model only gives rise to second-order phase transitions.

As we will show elsewhere,[7] the exclusive occurrence of second-order phase transitions is entirely due to two assumptions, (2.11) and (2.16), made here and by others[4,5] about the dependence of energy gap and lattice distortion energy on the asymmetry parameter ξ:

$$E_g(\xi) = E_c \cdot |g| \approx E_c(\tfrac{1}{2}ac - 3) \cdot |\xi| \quad \text{and} \quad \Delta E_l(\xi) = \tfrac{1}{2}V\kappa_\xi^{-1} \cdot \xi^2$$

When better expressions, such as

$$E_g(\xi) = E_c \cdot |g| \approx E_c \cdot \sinh((\tfrac{1}{2}ac - 3) \cdot |\xi|) \tag{3.4}$$

and

$$\Delta E_l \approx \frac{N}{2}(\mathrm{Br}_1^{-n} + \mathrm{Br}_2^{-n}) = \tfrac{1}{2}\mathrm{NB}(\tfrac{1}{2}\alpha)^{-n}((1-\xi)^{-n} + (1+\xi)^{-n}) \quad (3.5)$$

are used, first-order phase transitions also occur. For $n = 6$, an appropriate value for the repulsion exponent of the $TCNQ^- - TCNQ^-$ intrachain repulsion,[14] we find the *critical point* of the second-order phase transitions at $\kappa_{el}(0)/\kappa_\xi = 0.70$, with *second-order phase transitions* in the range $1 > \kappa_{el}(0)/\kappa_\xi \geq 0.70$ and *first-order* for $0.70 > \kappa_{el}(0)/\kappa_\xi > 0$.

(b) The non-symmetrical case

The non-symmetrical arrangement of the spatially extended $TCNQ^-$ ions about the stacking axis in RbTCNQ,[3] is outlined in figure 5. It is

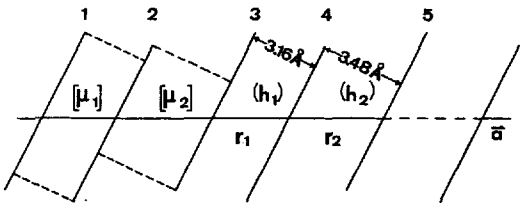

FIGURE 5 Principal characteristics concerning the stacking of the $TCNQ^-$ ions in a chain (RbTCNQ).

noteworthy that adjacent $TCNQ^-$ ions in this compound do not coincide completely looking along the normal to the planar quinoid skeletons (see figure 7 in reference 3). In order to account for this mismatch we introduce the coefficients μ_1 and μ_2 (see figure 5) with $0 \leq \mu_i \leq 1$; $\mu_i = 1$ denotes complete coincidence of the projections. It is assumed that the transfer integral h_i between neighbors as well as their repulsion energy is proportional to the coefficient μ_i between these neighbors. The expressions (3.4) and (3.5) now change into

$$E_g(\xi) = E_c \cdot |g| \quad \text{with } g = \sinh((\tfrac{1}{2}ac - 3)\cdot\xi - \tfrac{1}{2}\ln(\mu_2/\mu_1)) \quad (3.6)$$

$$\begin{aligned}\Delta E_l(\xi) &= \tfrac{1}{2}N(\mu_1\mathrm{Br}_1^{-n} + \mu_2\mathrm{Br}_2^{-n}) \\ &= \tfrac{1}{2}NB(\tfrac{1}{2}a)^{-n}u_1((1-\xi)^{-n} + (\mu_2/\mu_1)(1+\xi)^{-n}) \end{aligned} \quad (3.7)$$

In general, the lattice energy and deformation energy are no longer even functions of ξ, which means that in the expansion of $F(\xi, T)$ as a power series of ξ

$$F(\xi, T) = F_0 + \alpha(T)\cdot\xi + A(T)\xi^2 + B(T)\cdot\xi^3 + C(T)\cdot\xi^4 + \cdots. \quad (3.8)$$

the odd order terms are *not* identically zero by symmetry.

As a function of temperature, we only consider displacements of $TCNQ^-$'s (figure 5) parallel to the stacking axis, which leave μ_2/μ_1 practically constant. No change of symmetry takes place and according to Landau[6] only first-order phase transitions (discontinuous change in the distortion) or continuous changes are possible. However, if the shift

$$1 - \mu \equiv 1 - \mu_2/\mu_1 \tag{3.9}$$

equals zero, we arrive again at the symmetrical case, depicted in figure 1 and treated in the preceding sections.

IV. DETAILED TREATMENT

(a) The low temperature crystal structure of RbTCNQ

Crystalline RbTCNQ exhibits a pronounced first-order phase transition[2] at 376°K and in this section the preceding calculations, including thermal expansion and lattice vibrations, will be applied to its known crystal structure at 113°K, as determined recently by Hoekstra, Spoelder and Vos.[3] Apart for some preliminary structural investigations on KTCNQ,[8,3] it is the only known complete X-ray diffraction study of an (1:1) alkali$^+$ $TCNQ^-$ salt.

1) The symmetry of RbTCNQ is monoclinic and the material belongs to the space group of $P2_1/c$. The molecular volume is 287Å^3. Fairly isolated rows of $TCNQ^-$ ions along the **a**-axis are surrounded by Rb^+ ions, which are also stacked along the **a**-axis. In both rows alternating distances between neighboring ions appear. Figure 5 schematically shows the stacking of the shifted $TCNQ^-$ ions within such a row. Actually, the TCNQ's have the shape of a shallow boat, because their quinoid rings bend towards one another, whereas the $-C(CN)_2$ "tails" are pushed apart.[3] In this respect, it is noteworthy that theoretical calculations by Jonkman and Kommandeur[10] for the $TCNQ^-$ ion reveal that the greater part of the spin density (or "valence electron"), determining the electronic binding energy, is carried by the planar quinoid rings, whereas most of the negative charge is located on the $-C(CN)_2$ "tails" (see figure 1 in paper I).

2) Another interesting feature is the coordination of each Rb^+ ion by a distorted cube consisting of eight partially negatively charged nitrogen atoms from the $-C(CN)_2$ groups at almost equal distances (d_i = 3.04 ± 0.06Å) from the alkali$^+$ ion.[3] These distances are almost equal to the sum of the van der Waals radii: $r(Rb^+)$ = 1.5Å, $r(N)$ = 1.5Å.[15] Figure 3 of reference (3) gives a projection of the RbTCNQ structure along the **a**-axis. In a simplified representation, a Rb^+ ion is the centre of a cube with

eight nitrogen atoms $N_1 \cdots N_9$, belonging to different $TCNQ^-$ ions, at the angles. Obviously, the positions of the Rb^+ ions are mainly determined by the intrachain Rb-N repulsive forces within the (distorted) cube. The interionic Rb^+–Rb^+ distances in the **a**-direction are alternately 3.48Å and 3.73Å, and thus appreciably larger than twice the non-bonded ionic radius of Rb^+. We can therefore consider the RbTCNQ structure as relatively "soft" TCNQ chains supported on the perimeter by "hard" (Rb–8N) cubes.

3) From the unit cell dimensions at 113°K and room temperature, also determined by Hoekstra, Spoelder and Vos,[3] we calculate $\Delta a/a = 1.6\%$ and $\Delta b/b \approx \Delta c/c = 0.4\%$ over this temperature interval. The anisotropic expansion of the crystal can be considered as completely due to an isotropic expansion of the (Rb–8N) cubes, just discussed. Throughout this section we therefore use

$$\Delta a/a = \tfrac{2}{3}\Delta V/V \tag{4.1}$$

For the same reason, we expect about the same ratio between the linear compressibility κ_l (in the **a**-direction) and the volume compressibility κ_V.

4) From the thermal analysis of RbTCNQ at 113°K it looks reasonable to describe the vibrational motion of the Rb^+ and $TCNQ^-$ ions as isotropic with r.m.s. displacements of 0.115Å and 0.10Å, respectively. The Debye temperature Θ of the Rb^+- and $TCNQ^-$-sublattice is related to this r.m.s. displacement via the Debye–Waller factor[16]

$$\text{for } T \gtrsim \Theta \quad \overline{x^2} = 3\hbar^2 T/(mk\Theta^2), \tag{4.2}$$

from which one calculates

$$\Theta_0(Rb^+) = 120°K \quad \text{and} \quad \Theta_0(TCNQ^-) = 85°K \tag{4.3}$$

(b) Deformation energy of the rigid ionic lattice

Three major contributions to the lattice energy should be visualized, viz. the electrostatic Madelung energy $U_M(V, \xi)$, the repulsion energy within a $TCNQ^-$ chain $U_{rep}^{intra}(V, \xi)$ and the repulsion energy between neighboring $TCNQ^-$ and Rb^+ chains $U_{rep}^{inter}(V, \xi)$. The expansion of the crystal will be governed by the dimensionless parameter Δ, by which the linear expansion along the stacking (**a**-) axis is described

$$a = a_0 e^{\Delta} \tag{4.4}$$

and so for the volume expansion of the crystal by (4.1). Throughout this section we use the index 0 for quantities, derived from the low temperature crystal structure of RbTCNQ, which implies $\Delta \equiv 0$ at $T_0 = 113°K$.

1) For the calculation of $U_M(\Delta, \xi)$ and $U_{\text{rep}}^{\text{inter}}(\Delta, \xi)$ an accurate expression for the positions of the Rb^+ ions as a function of ξ and Δ is a necessity. Let us consider again the Rb-8N cubes. The positions of the eight nitrogen atoms are fixed at given ξ and Δ, if we assume that small changes in the distortion of a $TCNQ^-$ chain only take place parallel to the stacking axis, with an equal displacement for each constituent atom. This assumption looks reasonable because of the stable repulsive configuration due to the octahedrally surrounded Rb^+ ions. Now, the Rb^+ positions can obviously be found by minimizing the repulsion energy between the Rb^+ ion and the eight N-atoms with respect to the variable Rb^+ position

$$\sum_{i=1}^{8} d_i^{-p}(Rb^+ - N) = \text{minimum} \tag{4.5}$$

The distances d_i were determined from ξ, Δ and the exact nitrogen atomic coordinates.[3] The interchain repulsive exponent was taken as $p \approx 8$.[14] Inclusion of both Rb^+ neighbors of Rb^+ in (4.5) gives a small correction. Application of this method to the actual structure at 113°K leads to a deviation of the calculated Rb^+ positions from experiment of 0.08Å and in $\bar{d}_i$ of 0.002Å. We thus have a relation for the Rb^+ positions as a function of ξ and Δ as well as the dependence of $U_{\text{rep}}^{\text{inter}}(\Delta, \xi)$ on these parameters. The ξ-dependence in the range $-0.07 \leq \xi \leq 0.07$ is expressed in a quadratic form; the result is written as follows

$$U_{\text{rep}}^{\text{inter}}(\Delta, \xi) = NB_p(\bar{d}_i(\Delta))^{-p}\{1 + R_1\xi - R_2\xi^2\} = NB'_p(a(\Delta))^{-qp} \cdot \{f_p(\xi)\} \equiv N\Lambda(\Delta) \cdot f_p(\xi) \tag{4.6}$$

with

$$\Lambda(\Delta) = \Lambda_0 e^{-qp\Delta} \tag{4.7}$$

and

$$(\Delta\bar{d}_i/\bar{d}_i)_\xi = q \cdot \Delta a/a = q \cdot \Delta \tag{4.8}$$

Numerical results, computed from the RbTCNQ structural data, are

$$R_1 = 0.92 \quad \text{and} \quad R_2 = 3.3 \tag{4.9}$$

The coefficient R_1 should depend on μ and will be proportional to the shift $(1 - \mu)$ in a first approximation. Like R_1 and R_2, the exponent q is almost independent of the chosen p-value and amounts to

$$q \approx 0.65 \tag{4.10}$$

calculated from expansion data.

For the time being, Λ_0 remains an undetermined quantity.

2) The Madelung energy of the RbTCNQ crystal was evaluated by taking into account the partial charges on the $TCNQ^-$ ion, as calculated by Jonkman and Kommandeur[10] and as given in paper I, figure 1; the positions of the Rb^+ ions were determined by (4.5). The results are written in the form

$$U_M(\Delta, \xi) = -NA(\xi)e^2V^{-1/3m} \equiv -NM(\Delta) + NM'(\Delta)\cdot(\xi - \xi_M)^2 \quad (4.11)$$

with

$$M(\Delta) = M_0 \cdot e^{-1/2m\Delta} \quad \text{and} \quad M'(\Delta) = M'_0 \cdot e^{-1/2m\Delta} \quad (4.12)$$

and

$$(\Delta U_N/U_M)_\xi = -\tfrac{1}{2}m \cdot \Delta a/a = -\tfrac{1}{2}m \cdot \Delta \quad (4.13)$$

Computer calculations give the following results for RbTCNQ

$$\xi_M = 0.095 \quad (4.14)$$

at which distortion the minimum in $U_M(\xi)$ is reached. ξ_M should depend on μ in an analogous way as R_1.

The energies M_0 and M'_0 amount to

$$M_0 = 4.85 \text{ eV} \quad \text{and} \quad M'_0 = 1.57 \text{ eV} \quad (4.15)$$

The exponent m was calculated from expansion data

$$m \approx 1.00 \quad (4.16)$$

which reproduces the familiar $V^{-1/3}$ dependence of the Madelung energy. ξ_M, M, M' and m prove to be almost independent of p, chosen for the determination of the Rb^+ positions.

3) The repulsion between neighboring $TCNQ^-$ ions within a chain is given by (3.7) and rewritten in a slightly different form

$$U_{\text{rep}}^{\text{intra}}(\Delta, \xi) = \tfrac{1}{2}NB_n(\tfrac{1}{2}a)^{-n}\mu_1\{(1 - \xi)^{-n} + \mu(1 + \xi)^{-n}\} \equiv \tfrac{1}{2}N\Omega(\Delta)\cdot\{f_n(\xi)\} \quad (4.17)$$

where

$$\Omega(\Delta) = \Omega_0 \cdot e^{-n\Delta} \quad (4.18)$$

Ω_0 naturally cannot be evaluated from the RbTCNQ structure, but μ_1 and μ_2 can be estimated from geometrical projections of neighboring TCNQ's on a plane parallel to the molecular planes (figure 7 in reference 3), resulting in $\mu_1 \approx 0.56$, $\mu_2 \approx 0.30$ and $\mu \approx 0.54$.

Referring to (4.11), (4.17) and (4.6), the deformation (free) energy of the rigid ionic lattice now reads

$$F_l(\Delta, \xi) = -NM(\Delta) + NM'(\Delta)\cdot(\xi - \xi_M)^2 + \tfrac{1}{2}N\Omega(\Delta)\cdot f_n(\xi) + N\Lambda(\Delta)\cdot f_p(\xi) \quad (4.19)$$

(c) Free energy of lattice vibrations

The dependence of the free energy of lattice vibrations $F_{vib}(\Delta, \xi, T)$ on Δ and ξ will only be treated in an approximative, averaged manner. The sum of free energies in the $3N$ lattice modes in each of both (Rb^+ and $TCNQ^-$) sublattices is given by the conventional statistical mechanics of Bose-Einstein oscillators[16]

$$F_{vib}(\Delta, \xi, T) = kT \sum_{Rb, TCNQ} \sum_{i=1}^{N} \sum_{pol.} \ln (2 \sinh (\hbar w_{q_i}/2kT)) \tag{4.20}$$

In order to account for effects of anharmonicity, we make the usual assumption that a change of volume ΔV gives rise to the same relative change of frequency of every mode[16]

$$\Delta w_{q_i}/w_{q_i} = -\gamma \cdot \Delta V/V = -\tfrac{3}{2}\gamma \cdot \Delta \tag{4.21}$$

where γ is the Grüneisen constant, averaged over the longitudinal and transverse modes in both sublattices.

The dependence of F_{vib} on the alternation ξ within a chain is very small. The frequency change in the symmetry-split phonon bands is assumed to be given by a relation analogous to (4.21), viz.

$$\Delta w_{q_i}/w_{q_i} = \pm\gamma\xi \tag{4.22}$$

This expression is mainly of interest for the $TCNQ^-$ sublattice, because the alternation in a Rb^+ chain, as determined by (4.5), turns out to be exclusively dependent on the shift $(1 - \mu)$ of the $TCNQ^-$'s within a chain and not on the alternate distances between them; $\xi(Rb^+\text{-chain}) \approx \xi_\mu$, given by (4.41).

In the Debye approximation, the lattice spectrum takes the form

$$D(w)\,dw = 3w^2 w_D^{-3}\,dw$$

with $\hbar w_D = k\Theta$ and for temperatures above the Debye temperature (4.20) is approximated by

$$\begin{aligned} F_{vib}(\Delta, \xi, T) &\approx 3NkT \sum_{Rb, TCNQ} \int_0^{w_D} D(w) \ln(\hbar w/kT)\,dw \\ &= 3NkT \sum_{Rb, TCNQ} \{\ln(\Theta(\Delta)/T) - \tfrac{1}{3} - \tfrac{1}{2}\gamma^2\xi^2\} \end{aligned} \tag{4.23}$$

with

$$\Delta\Theta/\Theta = -\gamma \cdot \Delta V/V = -\tfrac{3}{2}\gamma \cdot \Delta \tag{4.24}$$

γ will be calculated later by application of the condition for equilibrium to the crystal at T_0 and room temperature; it is taken to be equal for the two chains.

(d) Electronic free energy

In a stoichiometric crystal, the electronic free energy of the originally unpaired π-electrons on the $TCNQ^-$ ions can be derived from the partition function Z_{el} of the bandsystem (2.20) and the expression for the band energies (2,4), leading to

$$F_{el}(\Delta, \xi, T) = -(2/\pi)NE_c \int_0^{\pi/2} [(g^2 + \cos^2(\tfrac{1}{2}ak))^{1/2} + (2kT/E_c)\ln(1 + \exp\{(-E_c/kT)\cdot(g^2 + \cos^2(\tfrac{1}{2}ak))^{1/2}\})]\, d(\tfrac{1}{2}ak) \tag{4.25}$$

For computational convenience we looked for an analytical expression for $F_{el}(\Delta, \xi, T)$. In the appendix we derive

$$F_{el}(\Delta, \xi, T) \approx -NE_c(g^2 + \tfrac{1}{2})^{1/2} - 2NkT\cdot\exp\{-(E_c/kT)(g^2 + \tfrac{1}{2})^{1/2}\} \cdot\{1 + (E_c/48kT)(g^2 + \tfrac{1}{2})^{-3/2}\}\cdot I_0((E_c/4kT)(g^2 + \tfrac{1}{2})^{-1/2}) \tag{4.26}$$

where $I_{0,1}(z)$ is a (zeroth, first order) modified Bessel function of the first kind. This expression should be compared with (2.22) derived for the simplified case. Some useful substitutions are

$$G \equiv 1 + 2g^2, \qquad Q \equiv (E_c/kT)(g^2 + \tfrac{1}{2})^{1/2} = (E_c/kT)(\tfrac{1}{2}G)^{1/2}, \tag{4.27}$$

and

$$s \equiv 1 + (E_c/48kT)(g^2 + \tfrac{1}{2})^{-3/2} = 1 + Q/12G^2, \qquad z \equiv (E_c/4kT)(g^2 + \tfrac{1}{2})^{-1/2} = Q/2G \tag{4.28}$$

which transfers (4.26) into

$$F_{el}(\Delta, \xi, T) \approx -NkT(Q + 2s\cdot e^{-Q}\cdot I_0(z)) \tag{4.29}$$

The volume and distortion dependence of F_{el} is determined by the Δ- and ξ-dependence of the bandparameters E_c and g via both transfer integrals, which are taken proportional to $\mu_{1,2}$ (figure 5). In the static lattice h_1 and h_2 follow from (2.8)

$$h_{1,2}(\Delta, \xi) = \mu_{1,2}h_0\cdot e^{3\Delta}(1 \mp \xi)^3 \exp\{\tfrac{1}{2}a_0c(1 - (1 \mp \xi)\cdot e^{\Delta})\} \tag{4.30}$$

These expressions were obtained by writing the π-electron wavefunctions as atomic $2p\sigma$-functions. In this approximation

$$h_0 = \tfrac{1}{6}(\tfrac{1}{2}Z')^4(\tfrac{1}{2}a_0/a_0')^3\cdot\exp(-\tfrac{1}{2}a_0c) \tag{4.31}$$

However, the transfer integrals are modified by lattice vibrations, which will be treated in a classical way ($T > \Theta$). Say, $u_1(\Delta, \xi, T)$ and $u_2(\Delta, \xi, T)$ are the amplitudes of the random-phase vibrations of the $TCNQ^-$'s, related to the amplitude $u(\Delta, T)$ in the undistorted lattice by

$$u_{1,2}(\Delta, \xi, T) = u(\Delta, T)\cdot(1 \mp \xi) \tag{4.32}$$

Now, r_1 and r_2 become time dependent and averaging over all phase differences, we are left with

$$r_{1,2}(t) = r_{1,2} \mp u_1 \sin \omega_1 t \quad \text{and} \quad r_{1,2}(t) = r_{1,2} \pm u_2 \sin \omega_2 t \tag{4.33}$$

each during half a period. Insertion of the expressions (4.33) into (2.8), followed by integration over time leads to the time-averaged transfer integrals $\bar{h}_1$ and $\bar{h}_2$:

$$\overline{h_{1,2}}(\Delta, \xi, T) = h_{1,2}(\Delta, \xi) \cdot (1 + t_{1,2}(\Delta, \xi, T)) \tag{4.34}$$

where

$$t_{1,2}(\Delta, \xi, T) = \tfrac{1}{4}uc\{uc \mp 2\gamma\xi \mp \gamma\xi(uc)^2 - 12u/a\} \tag{4.35}$$

Finally the behavior of $u(\Delta, T)$ with volume and temperature follows from (4.2) and (4.24)

$$u(\Delta, T) = \tfrac{1}{2}a_0(A_0 T)^{1/2} \cdot e^{3/2\gamma\Delta} \tag{4.36}$$

with $A_0 = 24\hbar^2/ma_0^2k\Theta_0^2(\mathrm{TCNQ}^-)$ ($\approx 1.75 \times 10^{-5}\mathrm{°K}^{-1}$ in RbTCNQ).

The bandparameters E_c and g are now easily found from (4.34)

$$E_c(\Delta, \xi, T) = 2(\bar{h}_1\bar{h}_2)^{1/2} = E_c^0 e^{3\Delta}(1 - \xi^2)^{3/2} \cdot \exp\{\tfrac{1}{2}a_0 c(1 - e^{\Delta})\} \cdot (1 + t) \tag{4.37}$$

with

$$t(\Delta, T) = \tfrac{1}{2}\{t_1(\Delta, \xi, T) + t_2(\Delta, \xi, T)\} = \tfrac{1}{4}(uc)^2(1 - 6/\tfrac{1}{2}ac) \tag{4.38}$$

and

$$\begin{aligned} g(\Delta, \xi, T) &= \sinh\{\tfrac{1}{2}\ln(\bar{h}_1/\bar{h}_2)\} \\ &= \sinh\{(\tfrac{1}{2}ac - 3 - \tfrac{1}{2}\gamma uc(1 + \tfrac{1}{2}(uc)^2)(1 + t)^{-1}) \cdot \xi - \tfrac{1}{2}\ln(\mu)\} \end{aligned} \tag{4.39}$$

These formulas clearly reveal that just like the negligible ξ-dependence of E_c also the variation of g with volume is very small.

According to (4.39) and neglecting lattice vibrations, the single band situation is reached at

$$\xi \approx \tfrac{1}{2}(\tfrac{1}{2}ac - 3)^{-1} \ln \mu \tag{4.40}$$

which in general does *not* coincide with the minimum of the intra chain repulsion energy (4.17), given by

$$\xi \equiv \xi_\mu \approx \tfrac{1}{2}(n + 1)^{-1} \ln \mu \tag{4.41}$$

Numerical estimates of E_c^0 and g_0 in RbTCNQ can for instance be obtained from (4.30) and (4.31). With $a_0 = 6.64\text{Å}$, $\frac{1}{2}a_0 c = 10.7$, $\mu \approx 0.54$, $\mu_1 \approx 0.56$ and

$\xi_0 = 0.049$, we find to $E_c^0/k \approx 2080°K$ and $g_0 \approx 0.74$. Better estimates are obtained by writing the π-electron wavefunction φ for the unpaired electron on the radical ions as a linear combination of atomic $2p\sigma$-functions. The coefficients were taken from Jonkman and Kommandeur's results.[10] In this approximation both h-integrals were calculated for the known atomic positions in RbTCNQ^3 and the results are[17]

$$E_c^0/k \approx 2010°K \qquad \text{and} \qquad g_0 = 0.67 \tag{4.42}$$

Although both sets of results agree surprisingly well, we will not attach great value to the constant E_c^0, because it arises from the *absolute* values of both transfer integrals. However, the calculated *ratio* between h_1 and h_2 and the subsequent g_0-value is a much more reliable quantity. Furthermore, g_0 enables us to determine from (4.39) the shift $(1 - \mu)$ of the TCNQ$^-$'s within a chain more accurately, resulting in $\mu = 0.58$.

(e) Thermodynamic relations and (partial) derivatives

The temperature dependence of the equilibrium distortion in one or more crystalline phases can be found by applying at each temperature the thermodynamic equilibrium condition

$$(\partial F(\Delta, \xi, T)/\partial \xi)_{\Delta, T} = 0 \tag{4.43}$$

along with the relation

$$(\partial F(\Delta, \xi, T)/\partial \Delta)_{\xi, T} = -\tfrac{3}{2}PV, \tag{4.44}$$

which is vanishingly small if we consider the crystal under normal conditions.

The determination of the partial derivatives of the total free energy with respect to ξ and Δ is a considerable task, but it is straightforward from the relations given in the preceding subsections. After tedious calculation, we find from (4.19), (4.20) and (4.29), differentiated with respect to ξ

$$N^{-1}\left(\frac{\partial F_l}{\partial \xi}\right)_{\Delta} = 2M'(\xi - \xi_M) + \tfrac{1}{2}n\Omega\{(1 - \xi)^{-n-1} - \mu(1 + \xi)^{-n-1}\} + \\ + \Lambda(R_1 - 2R_2\xi) \tag{4.45}$$

$$N^{-1}\left(\frac{\partial F_{\text{vib}}}{\partial \xi}\right)_{\Delta, T} = -3\gamma^2 \xi kT \tag{4.46}$$

$$N^{-1}\left(\frac{\partial F_{el}}{\partial \xi}\right)_{\Delta,T} = -E_c \cdot g\sqrt{\frac{G+1}{G}}$$
$$\cdot\left[1 - 2e^{-Q}I_0(z)\left\{\frac{1}{4G^2} + s\left(1 + \frac{1}{2G}\frac{I_1(z)}{I_0(z)}\right)\right\}\right]$$
$$\cdot\left[\tfrac{1}{2}ac - 3 - \tfrac{1}{2}\gamma uc(1 + \tfrac{1}{2}(uc)^2)(1+t)^{-1}\right] +$$
$$+ E_c\xi\sqrt{\tfrac{1}{2}G}$$
$$\cdot\left[1 - 2e^{-Q}I_0(z)\left\{\frac{-1}{12G^2} + s\left(1 - \frac{1}{2G}\frac{I_1(z)}{I_0(z)}\right)\right\}\right]$$
$$\cdot\left[3 + (\tfrac{1}{2}\gamma uc)^2(1 + (uc)^2)\right] \tag{4.47}$$

In the same way, differentiating with respect to Δ

$$N^{-1}\left(\frac{\partial F_l}{\partial \Delta}\right)_{\xi} = \tfrac{1}{2}mM - \tfrac{1}{2}mM'(\xi - \xi_M)^2 - \tfrac{1}{2}n\Omega \cdot f_n(\xi) - qp\Lambda \cdot f_p(\xi) \tag{4.48}$$

$$N^{-1}\left(\frac{\partial F_{vib}}{\partial \Delta}\right)_{\xi,T} = -9\gamma kT(1 - \tfrac{1}{2}\gamma^2(\xi^2 + \xi_\mu^2)) \tag{4.49}$$

$$N^{-1}\left(\frac{\partial F_{el}}{\partial \Delta}\right)_{\xi,T} = E_c\sqrt{\tfrac{1}{2}G}$$
$$\cdot\left[1 - 2e^{-Q}I_0(z)\left\{\frac{-1}{12G^2} + s\left(1 - \frac{1}{2G}\frac{I_1(z)}{I_0(z)}\right)\right\}\right]$$
$$\cdot\left[\tfrac{1}{2}ac - 3 - 4\gamma t(1+t)^{-1}\right] +$$
$$- E_c g\xi\sqrt{\frac{G+1}{G}}$$
$$\cdot\left[1 - 2e^{-Q}I_0(z)\left\{\frac{1}{4G^2} + s\left(1 + \frac{1}{2G}\frac{I_1(z)}{I_0(z)}\right)\right\}\right]$$
$$\cdot\left[\tfrac{1}{2}ac - \tfrac{3}{4}\gamma^2 uc(1 + \tfrac{3}{2}(uc)^2)(1+t)^{-2}\right] \tag{4.50}$$

Both sets of equations enable us, by application of (4.43) and (4.44), to determine implicitly the temperature behavior of the alternation and volume within one phase, if all quantities involved are known at one temperature. In the next subsection this will be shown for RbTCNQ. Anticipating these calculations about the phase transitions, we will make a few general remarks about their occurrence.

Continuous changes within one phase are easily detected by application of the formulas, just derived. However, a calculated discontinuity in ξ does

not correspond to a first-order transition, but to the disappearance of one phase (figure 8b) which must have been preceded by a first-order transition. The transition temperature and the temperature of disappearance only coincide in a critical transition. Generally, a total free energy calculation of both phases, over a certain temperature region, gives a decisive answer with regard to the first-order phase transition point, which is the temperature at which the two free energies are equal.

An explicit expression for $d\xi/dT$ will give more insight into the driving force of the changes within a phase. For simplicity, $d\xi/dT$ is only derived in the approximation of constant volume and negligible influence of lattice vibrations upon the transfer integrals. Defining the volume- and alternation compressibilities κ_V and κ_ξ of the rigid, ionic lattice by

$$\kappa_V^{-1} \equiv V(\partial^2 F_l/\partial V^2)_\xi = 4/g(N/V)\{-\tfrac{1}{4}m^2M + \tfrac{1}{4}m^2M'(\xi - \xi_M)^2 + \tfrac{1}{2}n^2\Omega \cdot f_n(\xi) + q^2p^2\Lambda f_p(\xi)\} \tag{4.51}$$

and

$$\kappa_\xi^{-1} \equiv V^{-1}(\partial^2 F_l/\partial \xi^2)_\Delta = (N/V)\{2M' + \tfrac{1}{2}n(n+1)\Omega((1-\xi)^{-n-2} + \mu(1+\xi)^{-n-2}) - 2R_2\Lambda\}, \tag{4.52}$$

we arrive at the following expression for the temperature derivative of the equilibrium alternation

$$\begin{aligned} d\xi/dT = & -(\partial^2 F/\partial T \partial \xi)/(\partial^2 F/\partial \xi^2) \\ & \approx 3\gamma^2\xi - 2^{3/2}(\tfrac{1}{2}ac - 3)g(G+1)^{1/2}G^{-1}Q^2e^{-Q}I_0(z) \\ & \times V/kN\kappa_\xi - 3\gamma^2 T - 2^{-1/2}(\tfrac{1}{2}ac - 3)^2(E_c/k)(C^2+1)G^{-3/2} \\ & \times [1 + 2e^{-Q}I_0(z)\{(G^2-1)(G^2+1)^{-1} \\ & \times Q(1 + G^{-1}\cdot I_1(z)/I_0(z) + 5/3G^2) - 2\}] \end{aligned} \tag{4.53}$$

At low temperatures $d\xi/dT$ turns out to be negative, but very small due to the large positive denominator, consisting of two major contributions, derived from the deformation energy (first term) and the electronic energy (final term), which are of the same order of magnitude. At higher temperatures the strongly temperature dependent exponential term in the electronic contribution to the denominator plays a very important role. Merely due to temperature increase, a maximum amount of about 20% can be added to this electronic contribution. This effect is still enhanced by the simultaneous decrease of g. The difference between the first and third term in the denominator now becomes smaller and $\partial^2 F/\partial \xi^2$ versus temperature exhibits a minimum. A non-zero minimum corresponds to a continuous change in the equilibrium distortion, whereas $\partial^2 F/\partial \xi^2 = 0$ ($d\xi/dT = -\infty$) at $\xi \neq 0$ points to the disappearance of the phase considered, preceded by a first-order transition.

The heats of transition involved in such a first-order phase transition can also be calculated from the free energy and compared with experiment[2]

$$\Delta H = T_t \cdot \Delta S \tag{4.54}$$

The entropy of each phase can be calculated

$$\begin{aligned} S(\Delta, \xi, T) &= S_{\text{vib}}(\Delta, \xi, T) + S_{\text{el}}(\Delta, \xi, T) \\ &= -\partial/\partial T(F_{\text{vib}}(\Delta, \xi, T) + F_{\text{el}}(\Delta, \xi, T)) \end{aligned} \tag{4.55}$$

From (4.23) and (4.29) one finds for $T > \Theta$

$$S_{\text{vib}}(\Delta, \xi, T) = 3Nk \sum_{\text{Rb. TCNQ}} \{\ln(T/\Theta) + \tfrac{1}{2}\gamma^2\xi^2\} \tag{4.56}$$

$$\begin{aligned} S_{\text{el}}(\Delta, \xi, T) = NkQ(1 + t)^{-1}[t + 2e^{-Q}I_0(z)\{-1/12G^2 + \\ + s(1 - \tfrac{1}{2}G^{-1}I_1(z)/I_0(z))\}] + 2Nkse^{-Q}I_0(z) \end{aligned} \tag{4.57}$$

With these relations we are able to compute the entropy in both coexisting phases at the first-order transition point and thus the enthalpy change involved.

(f) Phase transitions and continuous changes in RbTCNQ-like structures

All quantities needed can be derived from the low temperature RbTCNQ structure at T_0 as mentioned earlier in this section, except Λ_0 (4.6), Ω_0 (4.17) and γ (4.21). However, these missing quantities can be evaluated by application of the conditions (4.43) and (4.44), as worked out in (4.45) to (4.50), to the low temperature (LT) situation along with the known expansion of the crystal at room temperature. The temperature behavior of the equilibrium distortion and volume is now determined by applying (4.43) and (4.44) at each chosen temperature. The other quantities can be calculated simultaneously at this temperature.

1) Because E_c^0 is considered insufficiently known, the above procedure is executed for various E_c^0 values. The resulting $g(T)$ curves are given in figure 6. Imposing the same initial conditions at T_0, it appears that for higher values of the transfer integrals the behavior of g as a function of temperature becomes more continuous. The calculations lead to continuous changes for $E_c^0/k \geq 1700°\text{K}$ and first-order phase transitions for $1475°\text{K} \leq E_c^0/k < 1700°\text{K}$, which are semiconductor-to-semiconductor transitions, because a bandgap is maintained at high temperatures, caused by the shift $(1 - \mu)$ of the TCNQ^- ions within a chain (section IIIb), which is considered unchanged in the high temperature (HT) phase. For temperatures not too near the transition or inflection point an almost constant bandgap may be expected in the

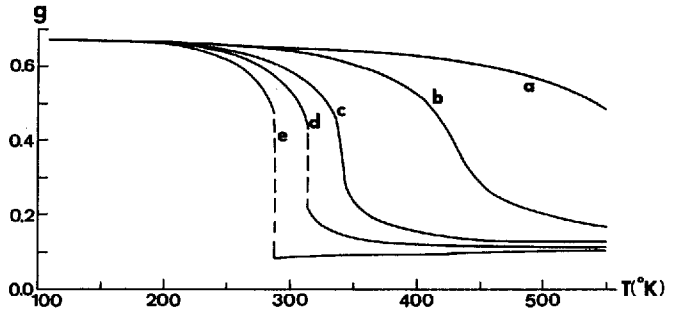

FIGURE 6 $g(T)$ curves, calculated for various E_c^0 values, starting with data from the low temperature structure of RbTCNQ, imposing $g = 0.67$ in each case.

E_c^0/k = 3000°K(a), 2100°K(b), 1700°K(c), 1600°K(d) and 1500°K(e).

LT phase as well as in the HT phase. Near a transition point, the g-value varies strongly in the LT phase, whereas the variation of g with T in the HT phase depends critically upon the sharpness of the transition. For $E_c^0/k <$ 1475°K a calculation of the total free energy at low temperatures reveals the instability of the presupposed LT.phase with regard to the HT phase.

In order to measure the influence of the electronic binding energy on the state of the lattice, it is interesting to determine the equilibrium positions Δ_1 and ξ_1 of the rigid, ionic lattice alone. Δ_1 and ξ_1 are easily calculated by application of (4.43) and (4.44) to the (free) energy F_1 of the ionic lattice, using (4.45) and (4.48). Such a calculation requires the knowledge of Ω_0 and Λ_0. As pointed out before, these quantities cannot be determined directly from the known LT structure. However, they can be evaluated indirectly by applying the thermodynamic conditions (4.43) and (4.44) to this structure, after having chosen a value for E_c^0. Therefore, in our calculations, Ω_0 and Λ_0, and consequently Δ_1 and ξ_1, will depend on the presupposed E_c^0-value. For given E_c^0, table I collects calculated values of Ω_0, Λ_0, γ, Δ_1 and ξ_1. Besides this, the compressibilities κ_γ and κ_ξ have been calculated from (4.51) and (4.52) at the equilibrium positions of the rigid, ionic lattice. A comparison of the values for Δ_1 and ξ_1, calculated for this case, with the *actual* structural data for RbTCNQ at low temperatures ($\Delta \equiv 0$, $\xi_0 = 0.049$) reveals that the presence of "valence" $2p\sigma$-electrons in the crystal effects a low temperature volume contraction of several percent and causes a distortion which deviates about 7% from ξ_1, the equilibrium distortion in the rigid, ionic lattice. Table I also gives the calculated transition temperature and the heat of transition, in case a first-order phase change is predicted (see figure 6).

As mentioned before, the first-order transition point is determined by a total free energy calculation in both phases. In figure 7 examples are given of

TABLE I

Calculated quantities in RbTCNQ-like crystal structures at given E_c^0 values. Explanation of symbols is given in the text.

E_c^0/k (°K)	Ω_0 (eV)	Λ_0 (eV)	γ	Δ_i	ξ_i	$\kappa_V \cdot 10^{11}$ (cm²/dyne)	$\kappa_\xi \cdot 10^{11}$	T_t (°K)	ΔH (col/mole)
1500	0.233	0.364	1.2	0.039	−0.030	3.6	2.6	284	78
1600	0.256	0.357	1.2	0.042	−0.029	3.6	2.5	314	64
1700	0.274	0.349	1.2	0.045	−0.028	3.6	2.4	continuous change	
1900	0.312	0.334	1.2	0.051	−0.026	3.7	2.2	continuous change	
2100	0.350	0.319	1.2	0.057	−0.025	3.7	2.1	continuous change	
2400	0.406	0.297	1.3	0.066	−0.023	3.7	1.9	continuous change	
3000	0.517	0.253	1.3	0.081	−0.022	3.8	1.7	continuous change	

free energy versus distortion curves at various temperatures, leading to (a) a continuous change and (b) a first-order transition. To facilitate these computations, the volume was kept constant. In the limited region of E_c^0 values, in which first order transitions occur, these transitions are almost critical, as illustrated in figure 7*b*.

2) An interesting speculative "experiment" is the replacement of the Rb^+ ion by a smaller alkali$^+$ ion, which affects especially the interchain repulsion

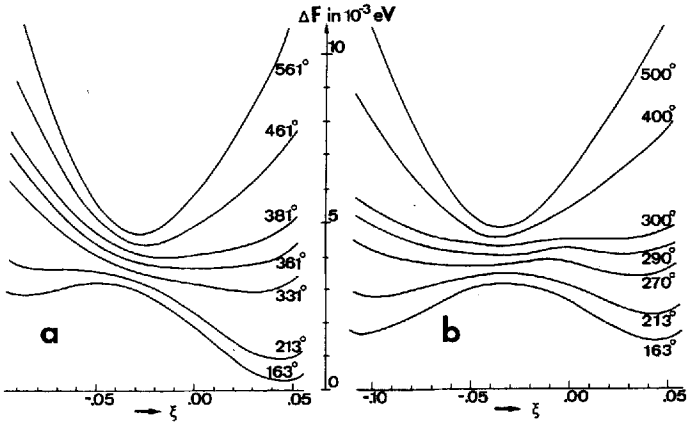

FIGURE 7 $F(\xi)$ curves, calculated at various temperatures (given in °K) from (4.19), (4.23) and (4.29) in the approximation of negligible crystal expansion.
a. $E_c^0/k = 1800$°K, leading to a continuous change in the semiconductor;
b. $E_c^0/k = 1600$°K, leading to a first-order transition.
The free energy shift of the various curves with respect to each other was chosen arbitrarily.

exponent p. As usual, we impose the condition that Λ_0 will increase slightly with decreasing p (smaller cation). Due to volume contraction, E_c^0 and Ω_0 will increase and g_0 decreases. Although E_c^0 and g_0 vary considerably with p, their product E_g^0 is hardly affected by p in these calculations. The result of a calculation of the variation of $E_c \cdot g$ (half the band gap) with temperature is depicted in figure 8. It is clear that the variation becomes smoother as p is taken to be smaller. This means that we expect less variation in the physical properties with temperature for the smaller counter ions. Substitution of ions larger than Rb^+, as for instance Cs^+, leads to instability of the LT phase of this crystal structure.

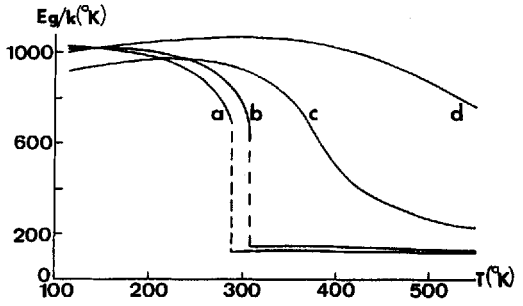

FIGURE 8 An attempt to determine the behavior of band gap with temperature in RbTCNQ-like crystal structures with different sizes of the cation, as reflected in varying values for the interchain repulsion exponent p. The $E_g(T)$ curves were calculated with
a. $p = 8$, $\Lambda_0 = 0.364$ eV, resulting in $E_c^0/k = 1500°K$, $\Omega_0 = 0.233$ eV;
b. $p = 7\frac{1}{2}$, $\Lambda_0 = 0.318$ eV, resulting in $E_c^0/k = 1800°K$, $\Omega_0 = 0.280$ eV;
c. $p = 6\frac{1}{2}$, $\Lambda_0 = 0.407$ eV, resulting in $E_c^0/k = 2620°K$, $\Omega_0 = 0.395$ eV;
d. $p = 5\frac{1}{2}$, $\Lambda_0 = 0.408$ eV, resulting in $E_c^0/k = 3600°K$, $\Omega_0 = 0.540$ eV.

3) We have also investigated the influence of the imposed low-temperature equilibrium distortion ξ_0 at T_0 as well as the influence of the shift $(1 - \mu)$ within a $TCNQ^-$ chain on the phase transitions in RbTCNQ-like crystal structures. Such variations of structural parameters predominantly affect the transition temperatures, but *not* the features of the calculated transitions. The case $\mu = 1$ naturally corresponds to the symmetrical case, discussed in section II and IIIa, leading to semiconductor-to-metal transitions. As found before,[7] these transitions are first- or second-order in nature, depending on the chosen E_c^0 value. It appears that Ω_0/E_c^0 is practically constant, whereas Δ_0/E_c^0 varies strongly with the imposed E_c^0 value.

V. COMPARISON WITH EXPERIMENT

In this section we compare the foregoing theoretical results with the experimental spin susceptibility behavior, heats of transition and temperature

dependent X-ray data for the (1:1) alkali$^+$ TCNQ$^-$ salts, including NH_4TCNQ. Methods for preparation of the crystalline materials and for measuring the quantities mentioned are given in paper I and reference 2.

On growing RbTCNQ crystals, a fibrous compound could also be collected. From an analysis for the elements, it turned out to be another (1:1) RbTCNQ salt ($C_{12}H_4N_4Rb$; calc. 29.5% Rb, 19.3%N; found 29.4%Rb, 19.2%N). This new compound will be denoted by RbTCNQ II.

Because the detailed treatment in the preceding section was based on the low temperature RbTCNQ structure, we first turn our attention to the LT phase of this compound. Although its experimentally observed first-order phase transition is not predicted exactly at 376°K in figure 6, a small change of e.g. the value of the exponent m in (4.11) from 1.00 into 1.10, which is within the experimental error, is sufficient to obtain a theoretical $g(T)$ curve, showing a sharp transition at 376°K with $E_c^0/k = 2100$°K (figure 9). For comparison,

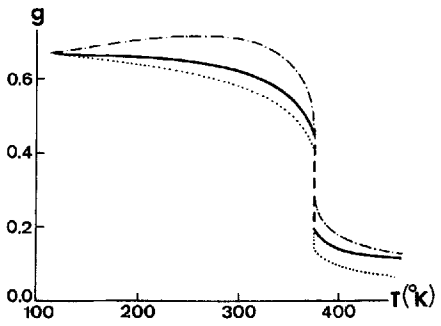

FIGURE 9 $g(T)$ curves with a sharp first-order transition at $T_t = 376$°K, as observed in RbTCNQ. ——: unapproximated calculation with $g_0 = 0.67$, $E_c^0/k = 2100$°K and $m = 1.10$. For comparison, the broken and dotted line are calculated without the influence of lattice vibrations on the transfer integrals and the effect of crystal expansion, respectively.

this figure also shows $g(t)$ curves, with a fixed transition temperature, calculated without the influence of lattice vibrations on the transfer integrals (broken line) or without the effect of crystal expansion (dotted line). Although the present E_c^0 value agrees almost completely with the calculated ones, mentioned at the end of section IVd, it predicts a spin susceptibility which is higher than experiment. As stated before, we do attach great value to the calculated $g(T)$ curves, but not to the absolute E_c^0 values, calculated indirectly. Therefore we choose an appropriate value for E_c^0/k (2725°K) and compare the calculated susceptibility curve, predicted by $g(T)$ from figure 9, with the experimental data. (figure 10). This comparison certainly enhances the credibility of the proposed model, as worked out in section IV.

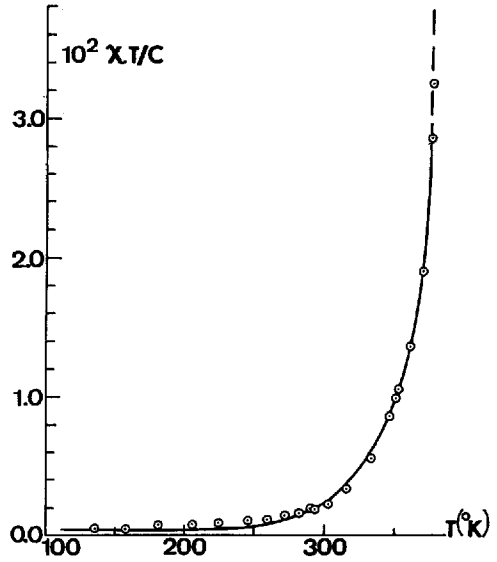

FIGURE 10 Comparison of theory with experimental susceptibility data for the low temperature phase of RbTCNQ. The drawn line gives a $\chi T/C$ versus T calculation with E_c^0/k = 2725°K, $\delta n = 0.0004$ and $g(T)$according to the fully drawn line in figure 9.

In the model we consider ξ as the one and only variable internal structural parameter. According to this, ξ becomes discontinuous in a first-order phase transition, which means a sudden displacement of the $TCNQ^-$'s parallel to the stacking axis. It is accompanied by a small volume contraction and a small enthalpy change (< 80 cal/mole, see table I). This prediction looks reasonable for the experimentally observed first-order tansitions in K TCNQ, NH_4TCNQ, RbTCNQ II and CsTCNQ, but certainly not for the RbTCNQ transition, in which much more heat is evolved (1010 cal/mole, see table II),

TABLE II

Transition data for the M^+TCNQ^- salts. The numbers in parentheses refer to the inflection point.of the $\chi(T)$curve (figure 14) for Na^+TCNQ^-, exhibiting a continuous change.

	T_i(°K)	$\chi T_i/C$	ΔH(cal/mole)	(phase) change
Li TCNQ	no phase transition or continuous change observed			
Na TCNQ	(345)	(0.034)	—	continuous
K TCNQ	396	0.082	60	first-order
NH_4 TCNQ	299	0.091	≈20	first-order
Rb TCNQ	376	0.105	1010	first-order
Rb TCNQ II	220	0.032	unobservable	first-order
Cs TCNQ	217	0.042	unobservable	first-order

whereas the structural change, as determined by temperature dependent X-ray diffraction on weakly powdered samples, is much more pronounced in RbTCNQ than in other salts. This is shown by the Guinier pictures of Rb^+-and e.g. Cs^+TCNQ^- in figures 11 and 12. Although these patterns are too complicated to analyze quantitatively, the drastic changes in RbTCNQ, as compared with those in CsTCNQ, are evident. Furthermore, in going through the phase transition from the low temperature side, we measured in RbTCNQ by microscopic investigation a minimum change in length along the needle axis of $\Delta a/a \approx +5.3\%$, which leads to a decrease of 33% in E_c and a transition heat of about 700 cal/mole, disregarding any structural changes. The crystals, however, often crack at the transition temperature, decreasing the accuracy of the measurement. If volume expansion should

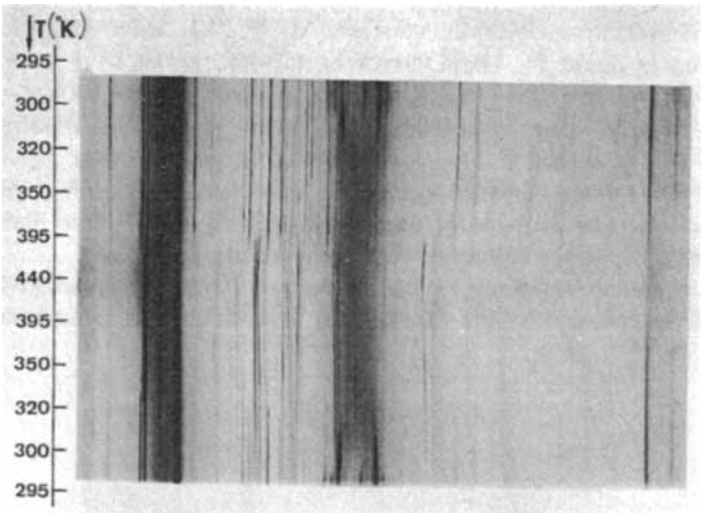

FIGURE 11 Temperature dependent X-ray diffraction pattern of a weakly powdered RbTCNQ sample, as measured with a Guinier camera. The pronounced phase transition as well as the large hysteresis in RbTCNQ is clearly shown.

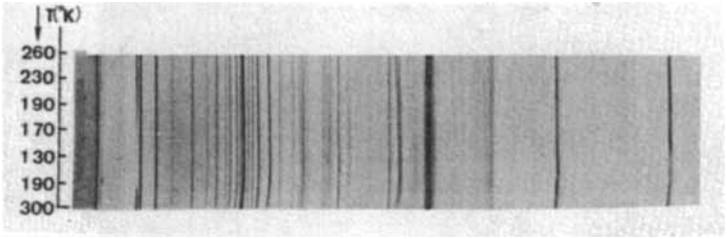

FIGURE 12 Guinier picture of powdered CsTCNQ, exhibiting a weak first-order phase change. Note the non-linear temperature scale.

account for the total heat effect, we calculate $\Delta a/a = +8.2\%$, resulting in $\Delta E_c/E_c = -47\%$, so that $E_c^0/k(\mathrm{LT}) = 2725°\mathrm{K}$ and $E_c^0/k(\mathrm{HT}) = 1450°\mathrm{K}$. However, this remains speculative, because little is known about the actual HT phase of RbTCNQ. In conclusion, we regard the first-order phase transition in RbTCNQ as a drastic, but unknown, structural change, which is induced by a continuous change in the LT phase, as considered before.

Table II collects some transition data for the M^+TCNQ^- salts: the transition (or inflection) temperature T_t, the number of free spins $\chi T_t/C$ midway the transition, the heat of transition ΔH and the nature of the (phase) change. The phase transitions were endothermic when the temperature was raised.

Figure 13 shows the Guinier picture of polycrystalline NaTCNQ. None of the diffraction lines exhibits a discontinuity, which is in accordance with the supposed continuous structural change with temperature in this salt. The experimental susceptibility curves of the M^+TCNQ^- salts, except LiTCNQ, are given in figure 14. These curves have been corrected for a Curie type "impurity"-content δn (given in table III), probably caused by non-stoichiometry or a small extent of disorder in the crystalline materials, discussed more extensively in paper I. The dashed curve shows the large hysteresis of RbTCNQ in going through the phase transition. The Guinier picture in figure 11 also clearly demonstrated this hysteresis. The original state can be regained by cooling the sample repeatedly in liquid nitrogen.

It is, of course, of interest to see, whether our calculations can qualitatively explain the influence of the counter ion, as evident from experiment. From

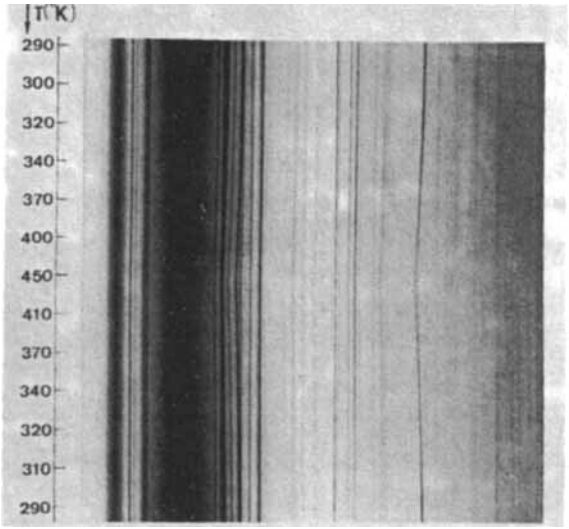

FIGURE 13 Guinier picture of polycrystalline NaTCNQ.

TABLE III

Three mutually dependent pairs of experimentally determined band parameters in a number of M^+TCNQ^- salts (HT phase, in case a phase transition occurs). The "impurity" contribution δn was determined from low temperature susceptibility data.

	LiTCNQ	CuTCNQ	NaTCNQ	KTCNQ	NH_4TCNQ	RbTCNQ	RbTCNQ II	CaTCNQ
g	0.66	0.20	0.38	~0.7	≈0.6–0.3*	≈0.3–0.1*	0.41	0.46
E_c/k	1185°K	2020°K	2170°K	~1300°K	~1000°K	~1200°K	1390°K	1180°K
E_b/k	635°K	1655°K	1500°K	~700°K	~600–800°K	~900–1100°K	930°K	760°K
E_a/k	780°K	405°K	820°K	≈900°K	~600–300°K	~350–100°K	570°K	540°K
$\lvert h_1\rvert/k$	1100°K	1235°K	1570°K	1250°K	~900–700°K	~800–650°K	1035°K	920°K
$\lvert h_2\rvert/k$	320°K	830°K	750°K	~350°K	~300–400°K	~450–550°K	465°K	380°K
δn	0.03	0.0005	0.006	0.0004	0.002–0.006	0.0004	0.0006	0.0004

* The g-value still varies continuously above the transition point.

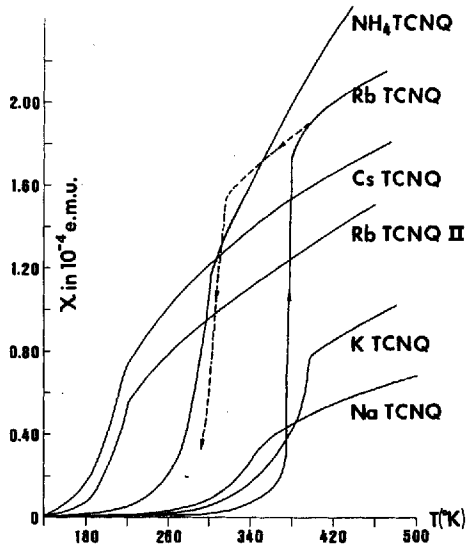

FIGURE 14 Experimental behavior of the spin susceptibility with temperature for a number of crystalline M^+TCNQ^- salts. A Curie type "impurity" content δn (table III) has been subtracted from each curve.

figure 8 it follows that a smaller ion with a smaller interchain repulsion exponent p, leads to a larger value of E_c^0 and to a smoother transition. From figure 6 it follows that a larger value of E_c^0 only, also leads to a smoother transition. It would, therefore, seem that the effect of the counter ion can be imitated by changing only the value of E_c^0 in the calculations, assuming larger values for smaller counter ions and keeping the crystal structure equal to that of RbTCNQ. Since the crystal structures of the other salts are as yet unknown, this appears to be the only legal procedure.

The results of such a calculation are given in figure 15, which should be compared with the experimental $\chi(T)$ curves of figure 14, It is obvious, that a reasonable imitation of the experimental behavior is obtained. Particularly in the series Rb^+, K^+, Na^+, Li^+TCNQ the sharpness of the transition (or the smoothness of the continuous change) is in good qualitative agreement. This is less so for RbTCNQ II and CsTCNQ, which may, however, have a different crystal structure, which would also follow from the instability calculated in subsection IVf.[2] Nevertheless, the essential features of the transition appear to be retained.

As shown in the figures 6 and 8, the $g(T)$ curves above the transition point bend more or less sharply toward a constant energy gap, which is maintained at higher temperatures due to the equilibrium situation at $\xi \neq 0$ for the rigid lattice. This gap extends the semiconductive behavior into the HT phase. This

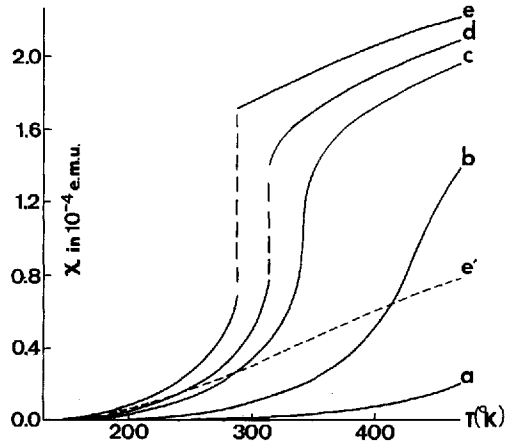

FIGURE 15 Calculated temperature dependence of the spin susceptibility for the various cases of figure 6. For comparison, the dahsed curve e' has been calculated with constant band parameters: $E_c/k = E_c^0/k = 1500°K$ and $g = g_0 = 0.67$.

is also demonstrated by the susceptibility of the M^+TCNQ^- salts at high temperatures. In figure 16, the number of unpaired electrons $\chi T/C$ versus temperature for Na-, K-, Rb(II)- and CsTCNQ in their HT phase is compared successfully with $\chi T/C$ curves, calculated from the band model with constant parameters. (See paper I for the unique determination of the relevant parameters). In the case of K TCNQ the temperature region is so

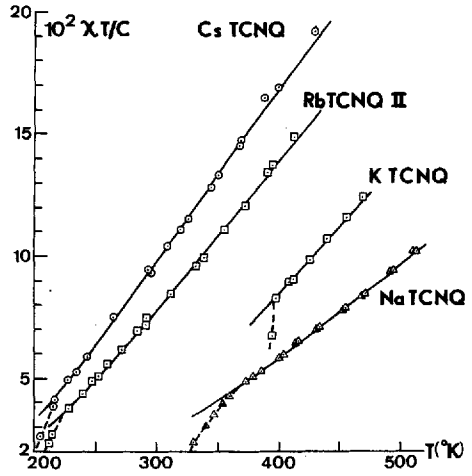

FIGURE 16 Comparison of experimental susceptibility data in the HT phase of a number of M^+TCNQ^- salts with $\chi T/C$ versus T curves, arising from a split-band system with constant band parameters, given in table III for the distinct salts.

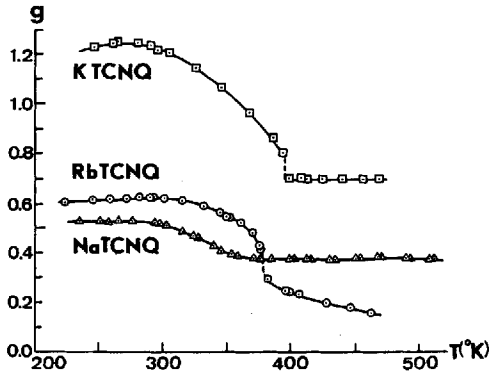

FIGURE 17 $g(T)$ curves, determined from experimental susceptibility data along with the following E_c values:
K TCNQ: $E_c/k = 1316°K$, RbTCNQ: $E_c^0/k = 2725°K$ (LT-phase) and 1450°K (HT-phase), NaTCNQ: $E_c/k = 2170°K$.

limited that only approximate values for the transfer integrals can be obtained. The measurements were continued up to the decomposition temperature of the materials. For RbTCNQ and NH_4TCNQ the effects of the transition appear to persist in the HT phase, as illustrated in the figures 17 and 18, where $g(T)$ curves are derived from experimental susceptibility data. The nonconstancy of the band parameters at high temperatures in Rb- and NH_4TCNQ prevents their precise numerical evaluation. Therefore, for RbTCNQ we used the earlier mentioned E_c^0 values for the LT and HT phase. The E_c value for NH_4TCNQ was chosen arbitrarily. In each salt, except RbTCNQ ,we assumed equal E_c values on both sides of the transition point. The resulting $g(T)$ curves in figures 17 and 18 are also in qualitative agreement with those, calculated in section IV and depicted in figures 6, 8 and 9. Finally, table III collects the (approximate) values of the band para-

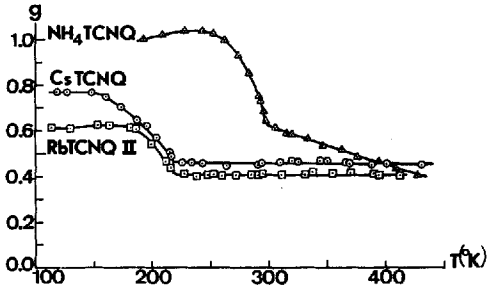

FIGURE 18 "Experimental" $g(T)$ curves, derived from the susceptibility behavior and undermentioned E_c-values:
NH_4TCNQ: $E_c/k = 1000°K$, CsTCNQ: $E_c/k = 1180°K$, RbTCNQ II: $E_c/k = 1390°K$.

meters in the HT phase of each M^+TCNQ^- salt under investigation, along with those for Li- and CuTCNQ, which have been treated earlier on the basis of the unperturbed one-dimensional split-band system (1.18).

VI. DISCUSSION

It is clear that in general the behavior of the simple TCNQ salts can be understood on the basis of the Bloch theory. The arguments for the applicability of the one electron bandsystem, set forth in paper I, obviously hold in every (1:1) alkali$^+$TCNQ$^-$ salt. However, it is quite imaginable that in other TCNQ salts the energy of the doubly occupied states is not quite as low as assumed here and consequently drastic changes in the behavior may be expected, as e.g. the occurrence of excitons and a completely different magnetic behavior, as reported by Chesnut and Phillips[19] and many others.[20] Concerning the properties of the TCNQ complexes, the nature of the counter cation[21] as well as the composition of the complex is determining. Evidence for the latter is, for instance, given by comparison of the simple Cs^+TCNQ^- salt (present study) with the triplet-exciton-containing $Cs_2^+(TCNQ)_3^-$ system, as studied by Chesnut and Arthur[22] and by comparing other TCNQ complexes of varying stoichiometry.[21,23] The alkali$^+$TCNQ$^-$ salts exhibit an intense ESR absorption at $g \approx 2$, with a width of a few Gauss. Apart from this central line, recent single crystal studies on Rb^+- and K^+TCNQ^- also reveal the occurrence of some electron-electron correlation in these salts, because of the observation of fine structure splittings[24] in the low susceptibility region at temperatures below 0°C. Probably, this phenomenon can be described as an electron-hole correlation, resulting in exciton states, which can coexist with the uncorrelated band system. On the other hand, in the above-mentioned exciton systems, like $Cs_2(TCNQ)_3$ and the morpholinium TCNQ complexes, it may become advantageous to start in the other limit instead of the Bloch theory and use the antiferromagnet as the zeroth-order approximation, as has been developed by Soos.[25]

The use of band theory calls for a discussion of the electrical conductivity. The alkali$^+$TCNQ$^-$ salts exhibit a semiconductive behavior with a d.c. conductivity in the range 10^{-4}–$10^{-5}\Omega^{-1}cm^{-1}$ and an activation energy of about 0.35 eV for Li^+-, Na^+-, K^+TCNQ^- and 0.18 eV for Cs^+TCNQ^-, all measured on compactions.[26,27,21] The conductivity in TCNQ salts is highly anisotropic and crystallographic results show that the high conductivity direction is parallel to the face-to-face stacks, in which the TCNQ's are arranged.[21] The activation energies, mentioned above, need not at all be equal to half the intrinsic energy gap. Especially in linear systems any structural disorder gives rise to localization of electronic states, leading to an

energy gap as far as d.c. measurements are concerned. Even in metallic one-dimensional systems d.c. conductivity measurements exhibit an energy gap of the order of 0.1 eV.[28] Accordingly, our preliminary investigations of a.c. conductivities in the limited range of 0–4 Mc/s on alkali$^+$TCNQ$^-$ crystals show a decreasing activation energy with increasing frequency. For LiTCNQ, for instance, the activation energy is reduced from 0.35 eV(d.c.) to 0.12 eV (4 Mc/s) and further reduction possibly occurs at still higher frequencies. Besides, the conductivity itself increases by about two orders of magnitude. Apart from the decrease in activation energy, we also mentioned in an earlier paper[2] the sudden increase in conductivity at the transition point for K TCNQ (by a factor of about 1.4) and RbTCNQ, in warming up these crystals. Experiments on the latter compound were hampered in connection with the breaking of the crystals in going through the transition. Let us calculate the increase of the effective numer of charge carriers from the split-band model.[29]

$$N_{\text{eff}} = \tfrac{1}{2}\pi^{-1} Na \int (m_e/m_k^*) f_k^0 \, \mathrm{d}k, \tag{6.1}$$

integrated over both bands. In this equation m_e and m^* are the free and effective electron mass, respectively, with $m_k^* = \hbar^2(\mathrm{d}^2E(k)/\mathrm{d}k^2)^{-1}$; f_k^0 is the Fermi-Dirac distribution function. Substituting the "experimental" band parameters for K TCNQ at T_t on both sides of the transition (figure 17), we calculate an increase in N_{eff} by a factor 1.5. The measured increase in σ obviously is entirely determined by the creation of more carriers during the phase transition. In the same way we predict from figure 17 in RbTCNQ an increase in σ by a factor 4.0.

Finally, we remark that the magnetic properties and processes involved in the phase transitions of the (1:1) alkali$^+$TCNQ$^-$ salts are very subtle and easily affected by, for instance, the size of the crystal. Microcrystalline K TCNQ, prepared by mixing dilute solutions of TCNQ and K I in acetonitrile at room temperature, exhibits an increased susceptibility by about a factor 5 at room temperature, whereas the phase transition of this sample was less pronounced. Crystalline RbTCNQ, ground to powder, did not even show the least trace of a phase change. The aggregate form of the sample influences its behavior noticeably. Irreproducible magnetic properties are observed in powder samples of M$^+$TCNQ$^-$ salts, in contrast with the reproducibility in crystalline material.

Phase transitions in TCNQ complexes under normal conditions were previously reported in the exciton-containing systems

$$[(C_6H_5)_3PCH_3]^+_{1-x}[(C_6H_5)_3AsCH_3]^+_x(TCNQ)_2^-$$

for $0 \leq x < 1$,[30,31] and in morpholinium $^+$TCNQ$^-$.[23]

In those cases the emphasis of the measurements has usually been on the triplet excitons, and no total susceptibility data are available. It is therefore not possible to apply the present theory to those compounds. It is worthwhile to note, however, that structural changes also seem to be dominant in governing those phase transitions.[23]

For the simple alkali-TCNQ salts, however, it appears that the present theory can be fruitfully applied.

Acknowledgements

The authors are grateful to A. Vos, A. Hoekstra and B. C. van Zorge for many useful discussions. Further we thank the staff of the Laboratory for Polymer Chemistry of this University for placing their Differential Scanning Calorimeter at our disposal and Tj. Hibma for performing the DSC-measurements. The authors are also indebted to J. H. Wiersma of the Department of Inorganic Chemistry of this University for providing the Guinier photographs. (The computations were carried out on a Telefunken TR4 computer, Computer Centre, University of Groningen).

APPENDIX

In section IVd the expression (4.25) for the electronic free energy as a function of volume, distortion and temperature was given. In order to find solutions Δ and ξ at a given temperature from the total free energy, the conditions (4.43) and (4.44) should be satisfied simultaneously. To facilitate computations and enhance physical insight, we transform (4.25) into an analytical approach, which should hold in the region of interest.

We approximate (4.25) in the following simplified manner, substituting $y \equiv ak$

$$F_{el}(\Delta, \xi, T) = -(2/\pi)NE_c\left[\int_0^{\pi/2} (g^2 + \cos^2(\tfrac{1}{2}y))^{1/2}\, d(\tfrac{1}{2}y) + \right.$$
$$\left. + (2kT/E_c)P \int_0^{\pi/2} \exp\{(-E_c/kT)(g^2 + \cos^2(\tfrac{1}{2}y))^{1/2}\}\, d(\tfrac{1}{2}y)\right] \tag{7.1}$$

where P is a numerical constant. The first integral (I_1) is a complete elliptic integral of the second kind, which can be approximated reasonably by

$$I_1 \approx \tfrac{1}{2}\pi(g^2 + \tfrac{1}{2})^{1/2} \tag{7.2}$$

for g-values not too near $g = 0$. However, for $g \approx 0$ a comment on I_1 has been made by us in a preceding paper,[7] which makes plausible the use of an expression like (7.2) also for small g-values.

The second integral (I_2) in (7.1) is written as follows, substituting $Q \equiv (E_c/kT)(g^2 + \frac{1}{2})^{1/2}$

$$I_2 = \tfrac{1}{2}\int_0^{\pi} \exp\{-Q(1 + \cos y/(2g^2 + 1))^{1/2}\, dy \tag{7.3}$$

Expanding the square root expression in the exponent, we find

$$I_2 \approx \tfrac{1}{2}e^{-Q}\int_0^{\pi} \exp(-Q \cos y/2G) \cdot \exp(Q \cos^2 y/8G^2)\, dy$$

$$\approx \tfrac{1}{2}e^{-Q}\int_0^{\pi} \exp(-Q \cos y/2G) \cdot (1 + Q \cos^2 y/\delta G^2)\, dy \tag{7.4}$$

with $G \equiv 1 + 2g^2$. Both terms in this integral are related to the zeroth- and first-order modified Bessel functions of the first kind, denoted by $I_0(z)$ and $I_1(z)$ respectively, which can be written down as a known series expansion.[32]

With $z \equiv Q/2G$

$$I_2 \approx \tfrac{1}{2}\pi e^{-Q} I_0(z)\{1 + (1 - z^{-1} \cdot I_1(z)/I_0(z))Q/8G^2\} \tag{7.5}$$

In the temperature region, where the I_2-term contributes noticeably to the electronic free energy, the correction term between the brackets becomes less important and can be simplified, resulting in

$$I_2 \approx \tfrac{1}{2}\pi e^{-Q} I_0(z)(1 + Q/12G^2) \tag{7.6}$$

Substitution of (7.2) and (7.6) into (7.1) leads to

$$F_{el}(\Delta, \xi, T) \approx -NE_c(g^2 + \tfrac{1}{2})^{1/2} - 2NkTPe^{-Q} I_0(z)(1 + Q/12G^2) \tag{7.7}$$

This expression for F_{el}, along with its derivative with respect to g was checked in the region of g- and E_c/T-values of interest and compared with the results from expression (4.25). A P-value near to unity (0.8–1.0) gives satisfactory results. If P is calculated through as a variable ($0.5 \leq P \leq 1.0$) in (4.47) and (4.50), it does not even affect the essential features forthcoming from our theoretical treatment, as embodied in section IVf. Therefore, we have simply taken $P = 1$ and arrive from (7.7) at formula (4.26) for $F_{el}(\Delta, \xi, T)$.

References

1. J. G. Vegter, J. Kommandeur and P. A. Fedders, *Phys. Rev.* **B1**, 2929 (1973).
2. J. G. Vegter, T. Hibma and J. Kommandeur, *Chem. Phys. Letters* **3**, 427 (1969).
3. A. Hoekstra, T. Spoelder and A. Vos, *Acta Cryst.* **B28**, 14 (1972).
4. D. Adler and H. Brooks, *Phys. Rev.* **155**, 826 (1967).
5. J. J. Hallers and G. Vertogen, *Phys. Rev.* **B4**, 2351 (1971).
6. L. D. Landau and E. M. Lifshitz, Statistical Physics, Chapter 14 (Pergamon Press, 1960).
7. J. G. Vegter and J. Kommandeur, *Phys. Rev.* **B** (1973) (in the press).
8. G. R. Anderson and C. J. Fritchie, paper presented to *Soc. for Appl. Spectry*, San Diego, October 1963.

9. P. A. Fedders and J. Kommandeur, *J. Chem. Phys.* **52**, 2014 (1970).
10. H. Th. Jonkman and J. Kommandeur, *Chem. Phys. Letters* **15** 496 (1972).
11. G. H. Wannier, Statistical Physics, Section 9.2 (Wiley, 1966).
12. Proceedings of the International Conference on the Metal-Nonmetal Transition, San Francisco, California, U.S.A., March 1968, *Rev. Mod. Phys.* **40**, 673–845 (1968).
13. C. Haas, *Phys. Rev.* **140**, A863 (1965).
14. A. J. Dekker, Solid State Physics, Section 5.4 (MacMillan Ltd., London, 1963).
15. L. Pauling, The Nature of the Chemical Bond, 3rd ed. p. 260 (Ithaca: Cornell Univ. Press, 1960).
16. J. M. Ziman, Principles of the Theory of Solids, Chapter 2 (Cambridge, Univ. Press, 1964).
17. B. C. van Zorge, private communication.
18. J. G. Vegter, P. I. Kuindersma and J. Kommandeur, Proceedings of the Second International Conference on Conduction in Low-Mobility Materials, Eilat, Israel (1971).
19. D. B. Chesnut and W. D. Phillips, *J. Chem. Phys.* **35**, 1002 (1961).
20. See, for instance, P. L. Nordio, Z. G. Soos and H. M. McConnell, *Ann. Rev. Phys. Chem.* **17**, 237 (1966) and references cited in this review.
21. W. J. Siemons, P. E. Bierstedt and R. G. Kepler, *J. Chem. Phys.* **39**, 3523 (1963).
22. D. B. Chesnut and P. Arthur Jr., *J. Chem. Phys.* **36**, 2969 (1962).
23. J. C. Bailey and D. B. Chesnut, *J. Chem. Phys.* **51**, 5118 (1969).
24. T. Hibma, P. Dupuis and J. Kommandeur, *Chem. Phys. Letters*, **15**, 17 (1972).
25. Z. G. Soos, *J. Chem. Phys.* **43**, 1121 (1965).
26. L. R. Melby, R. J. Harder, W. R. Hertler, W. Mahler, R. E. Benson and W. E. Mochel, *J. Am. Chem. Soc.* **84**, 3374 (1962).
27. R. G. Kepler, P. E. Bierstedt and R. E. Merrifield, *Phys. Rev. Letters* **5**, 503 (1960).
28. A. N. Bloch, R. B. Weisman and C. M. Varma, *Phys. Rev. Letters*, **28**, 753 (1972).
29. A. J. Dekker, Solid State Physics, Section 10.5 (McMillan Ltd, London, 1963).
30. R. C. Kepler, *J. Chem. Phys.* **39**, 3528 (1963).
31. Y. Iida, *Bull. Chem. Soc. Japan*, **43**, 3685 (1970).
32. M. Abramowitz and I. A. Stegun, Handbook of Mathematical Functions, Chapter 9 (Dover Publ., New York, 1965).